Volume 22, issue 11, November 2007 ISSN 0883-2927

ELSEVIER

Applied Geochemistry

JOURNAL OF THE INTERNATIONAL ASSOCIATION OF GEOCHEMISTRY

Continued on outside back cover

Available online at www.sciencedirect.com
ScienceDirect
Applied Geochemistry 22 (2007) 2344–2361
Applied Geochemistry
www.elsevier.com/locate/apgeochem

Estimating the longevity of limestone drains in treating acid mine drainage containing high concentrations of iron

Silvana Santomartino *, John A. Webb

Department of Earth Sciences, La Trobe University, Victoria 3086, Australia

Received 2 June 2004; accepted 7 April 2007
Editorial handling by B. Kimball
Available online 5 June 2007

Abstract

Limestone drains are often implemented in the treatment of acid mine drainage (AMD), but when the AMD contains high levels of dissolved Fe their lifetime is dependent on the rate of precipitation of Fe hydroxide on the limestone surface. This study used a small-scale laboratory experiment to define the longevity of a limestone drain by determining the thickness of the Fe coating encapsulating the limestone particles when the system lost its maximum neutralising potential. Synthetic AMD (100 mg/L Fe, pH 4–4.8) was pumped through a column containing limestone particles for 1110 h, when the effluent pH had dropped from a maximum of 6.45–4.9. The decline in neutralisation during the experiment was due to the formation of Fe hydroxide coatings on the limestone grains. These coatings are composed of lepidocrocite/goethite in three distinct layers: an initial thick porous orange layer, overlain by a dense dark brown crust, succeeded by a layer of loosely-bound, porous orange globules. After 744 h, a marked increase in the rate of pH decline occurred, and the system was regarded as having effectively failed. At this time the Fe hydroxide crust effectively encapsulated the limestone grains, forming a diffusion barrier that slowed down limestone dissolution. Between the coating and the limestone substrate was a 60 μm wide void, so that agitation of the limestone sample would readily remove the coating from the limestone surface.

In the experimental system, the time for sufficient Fe hydroxide to precipitate on the limestone to cause a distinct decline in the rate of neutralisation was defined by:

$$t\ (\text{years}) = \frac{\text{surface area } (\text{m}^2) \times 4.4}{\text{fraction Fe retained in system} \times [\text{Fe}^{2+}]\ (\text{mg/L}) \times \text{flowrate } (\text{L/h})}.$$

At this time the limestone in the drain would need to be replaced or mechanically agitated to remove the Fe hydroxide coating, to allow the system to continue functioning at its maximum potential. Application of this formula to the field situation shows that even when the influent Fe concentrations are moderately high, limestone drains will continue to function well for one to several years. Thus, passive limestone systems can be used in AMD treatment when the influent Fe concentration is considerably greater than 1 mg/L, the currently recommended limit, particularly given that the Fe precipitates armouring the limestone grains may be loosely bound and relatively easily dislodged. Therefore, limestone drains are more widely applicable than presently realised.

* Corresponding author. Present address: Golder Associates Pty. Ltd., Australia. Fax: +61 7 3721 5401.
E-mail address: ssantomartino@golder.com.au (S. Santomartino).

0883-2927/$ - see front matter © 2007 Elsevier Ltd. All rights reserved.
doi:10.1016/j.apgeochem.2007.04.020

1. Introduction

Acid mine drainage (AMD) forms when sulphide minerals (e.g. pyrite and pyrrhotite) are exposed to O_2 and/or Fe(III) during mining operations (Singer and Stumm, 1970). Oxidation and hydrolysis of the sulphides produce acidic waters (pH often <3) which may leach into local waterways and groundwater, along with elevated concentrations of SO_4^{2-}, Fe^{2+} and Fe^{3+}, as well as Al^{3+}, Mn^{2+}, Pb, Zn, Cd, and other metals, depending on the specific mineral deposit.

Limestone ($CaCO_3$) is a common reagent choice worldwide for the neutralisation of acid mine drainage as it is cost-effective, widely available and is often present in the local natural environment (Hedin et al., 1994; Nairn et al., 1991). The dissolution of one mole of $CaCO_3$ consumes one to two moles of acidity and may release alkalinity (as HCO_3^-) into solution (Garrels and Christ, 1965). Treatment of AMD with limestone can increase the pH to 6.0–7.5 (Pearson and McDonnell, 1975; Webb and Sasowsky, 1994), allowing the metals to be removed from solution via precipitation and sorption.

Limestone is commonly used in both active and passive AMD treatment. Active systems use some form of mechanical procedure to continuously add an alkaline reagent to reach a designated pH, whilst passive treatment techniques rely on in situ chemical and/or biological neutralisation without mechanical assistance. Passive treatment systems that rely exclusively upon limestone for neutralisation are generally implemented for post-closure, low-acid-load treatment scenarios (Taylor and Waters, 2003), and are relatively inexpensive to construct and maintain. They include anoxic and oxic limestone drains (Turner and McCoy, 1990), open limestone channels (Ziemkiewicz et al., 1997), limestone diversion wells (Arnold, 1991; Faulkner and Skousen, 1995) and vertical flow ponds or successive alkalinity producing systems (Kepler and McCleary, 1994; Rose, 2006). Limestone drains are closed trenches filled with limestone, through which the AMD percolates. They are designed to exclude O_2 within the trench, thereby inhibiting $Fe(OH)_3$ precipitation onto the limestone (described further below). Anoxic drains often have a pretreatment step to remove O_2 from the influent AMD, e.g. the initial section of the trench may be filled with organic material. In oxic limestone drains the influent AMD contains relatively high O_2 (in equilibrium with the atmosphere). Limestone drains, channels and diversion wells utilise limestone gravel to avoid clogging (Hedin et al., 1994; Robbins et al., 1999), although this reduces the reactive surface area compared to the very fine-grained limestone used in active systems.

During neutralisation of acid drainage a number of different minerals may precipitate. If SO_4^{2-} occurs in high concentrations in the AMD (>2000 mg/L; McDonald and Webb, 2005), gypsum ($CaSO_4 \cdot 2H_2O$) may form. Dissolved Fe(III) and Al will precipitate as metal hydroxides, including ferrihydrite ($Fe(OH)_3$) and gibbsite ($Al(OH)_3$); no O_2 is necessary for these reactions (Hedin et al., 1994):

$$Fe^{3+} + 3H_2O = Fe(OH)_3 + 3H^+ \quad (1)$$

$$Al^{3+} + 3H_2O = Al(OH)_3 + 3H^+ \quad (2)$$

The Fe^{2+} ion in acid drainage can precipitate as $Fe(OH)_3$ provided O_2 is present:

$$Fe^{2+} + H^+ + (1/4)O_2 = Fe^{3+} + (1/2)H_2O \quad (3)$$

$$Fe^{3+} + 3H_2O = Fe(OH)_3 + 3H^+ \quad (1)$$

Neutralisation of AMD with limestone removes H^+:

$$\text{for pH} > 6.4; \quad CaCO_3 + H^+ = Ca^{2+} + HCO_3^- \quad (4)$$

$$\text{for pH} <\sim 6.4; \quad CaCO_3 + 2H^+ = Ca^{2+} + H_2CO_3 \quad (5)$$

Removal of H^+ automatically favours the Fe precipitation reactions, so that limestone treatment of AMD will inevitably cause precipitation of ferric hydroxides around the limestone grains. Removal of O_2 from the AMD, as in anoxic limestone drains, will inhibit the rate of precipitation if Fe^{2+} is the dominant Fe species in solution.

Iron hydroxide precipitates have caused the failure of many passive limestone treatment systems by encapsulating the limestone grains and inhibiting further dissolution (Kepler and McCleary, 1994; Robbins et al., 1999); in addition, gibbsite can fill the interstitial spaces and clog the system (Cravotta and Trahan, 1999). To reduce the effect of precipitates and ensure the maximum lifetime of limestone passive systems, it has been recommended that Fe levels in the influent AMD should be below 1 mg/L (Hedin et al., 1994). Nevertheless, even at these low levels some precipitation of Fe will occur, and can affect the performance of a limestone system.

Limestone grains coated by precipitates are less effective at neutralising acid than uncoated particles, because the armouring limits the rate at which the

solid limestone is attacked by H^+ ions. Although armoured limestone can still cause a rapid increase in the pH of influent AMD (Cravotta and Trahan, 1999), this slows with time, and the neutralisation rate decays logarithmically (Ziemkiewicz et al., 1996). A coating of metal hydroxide can reduce the reactivity of limestone by a factor of 2.5–5 (Pearson and McDonnell, 1975; Ziemkiewicz et al., 1997).

The extent of armouring, measured by the thickness of the coating, has not been widely investigated. Visual examinations typically estimate the thickness as up to 1 mm (Cravotta and Trahan, 1999), but this is likely to be too high. Schwertmann and Friedl (1998) dissolved the Fe coatings on limestone particles in oxalate and/or dithionite–citrate–bicarbonate (DCB), and calculated the average minimum thickness of the ferrihydrite film as only 0.9–4.7 μm, assuming that the Fe hydroxide was non-porous and had a mean density of 4 g/cm. In constant flow experiments of AMD neutralisation, Hammarstrom et al. (2003) found the limestone grains to be coated in a rind of gypsum encapsulated by a 10–30 μm thick layer of Fe–Al hydroxysulfate.

Although the negative effect of armouring on the performance of passive limestone systems is well known, few studies to date have examined the relationship between the thickness of the Fe coatings and the decrease in neutralising potential of the limestone system. Sun (2000) developed an empirical model for calculating the expected lifetime of open limestone channels, taking into account limestone surface area and dissolved Fe concentration, but assuming the thickness and rate of development of the Fe coatings.

The aim of the present study is to develop a general relationship for the longevity of limestone drains from the average minimum thickness of the armouring and the elapsed time when the limestone loses its maximum neutralising ability. This indicates when the limestone in the drains would need to be replaced or the precipitates removed (e.g. via mechanical shaking) to prevent the system from failing. In addition, the mineralogy and morphology of the Fe precipitate and the strength of bonding to the limestone surface were examined.

2. Experimental system

The study used a small-scale laboratory limestone system consisting of a column filled with limestone gravel. To maintain continuously saturated conditions, synthetic AMD (pH 4–4.8, 100 ± 5 mg/L Fe) was directed upward through the column and the effluent was captured in a sealed carboy. The pH of the effluent was measured daily or more frequently and ion concentrations were measured periodically. The experiment was terminated after 46.2 days (1110 h) when the pH of the effluent solution had decreased from a maximum of 6.45–4.9, indicating that the neutralising ability of the system had failed. Limestone grains were then removed from the column and the thickness of the Fe coatings measured using microscope analysis (light and SEM). This was crosschecked against the amount of Fe precipitated in the column, from the difference in total Fe concentrations of the influent and effluent waters. The physical nature of the Fe coating and its adhesion to the limestone surface were also examined.

Initially, the influent solution was not sparged to remove O_2. However, oxidation of dissolved Fe^{2+} changed the pH of the synthetic AMD before it entered the column, so sparging with N_2 was necessary to largely remove the dissolved O_2. Thus, the O_2 levels in the column closely approximated those in an anoxic limestone drain for most of the experiment. Nevertheless, the results can be applied to oxic limestone drains and open limestone channels, as will be discussed further below.

2.1. Limestone

Microcrystalline limestone of high purity (98% $CaCO_3$) from Buchan, eastern Victoria, was used; a low dolomite content is required, as this mineral has slower reaction kinetics than calcite (Turner and McCoy, 1990). The limestone particles used in the experiment had a maximum length of 0.5–1.3 cm and a minimum length of 0.05–0.4 cm; the recommended diameter for limestone grains in passive treatment systems is 2.1–2.8 cm (Hedin et al., 1994) to 3–10 cm (Robbins et al., 1999). Limestone fines and particles less than 0.05 cm in diameter were removed, because small void spaces can become plugged by precipitates (Hedin et al., 1994). Limestone particles larger than 1.3 cm across were also removed because larger particles have a smaller surface area to volume ratio and hence are less reactive. The limestone was air-dried and stored at room temperature; 555 limestone particles were randomly selected, 50 of which were used to determine average surface area (see Section 2.6), and

the remainder, weighing 78.46 g, placed in the column.

2.2. Column

The small vertical column containing the limestone was a 6.5 cm diameter, 7 cm high PVC tube, threaded at both ends and capped with screw tops; a non-return sight valve for a swimming pool filtering system was used (Fig. 1). A piece of circular PVC plastic 50 mm in diameter and 6 mm thick with 3 mm holes drilled into it was placed at the base of the vertical tube to act as a filter. The synthetic AMD was pumped through the vessel at 2.75 mL/min, entering the base and exiting through the top.

2.3. Preparation of synthetic acid mine drainage

Analytical grade reagents were used to produce the synthetic AMD. Initially 10.5 μL of concentrated H_2SO_4 was added to a 25 L carboy and made up to volume with distilled water, giving a pH of 4.8; however, after the experiment had run for 524 h, the pH of the synthetic AMD was decreased to 4.0 (see reasoning below). Approximately 13.0 g of $FeSO_4 \cdot 7H_2O$ and 3.4 g of KCl were added to a 500 mL volumetric flask containing low pH water from the carboy. The flask contents were shaken to ensure the complete dissolution of the chemical salts before being poured back into the carboy, which was stirred thoroughly. The exact weight of $FeSO_4 \cdot 7H_2O$ added to each carboy was used to calculate accurately the concentration of Fe^{2+} present. Each carboy therefore contained a solution of 100 (±5) mg/L Fe^{2+} (0.045 mol/L Fe) and 70 (±3) mg/L K^+. Nine 25 L carboys containing the synthetic acid mine drainage were required for the experiment; in total 192.89 L of synthetic acid mine drainage were directed through the limestone column (78.98 L at pH 4.8 and 113.90 L at pH 4). The KCl added to the synthetic AMD was used as a tracer, as it did not take part in any of the reactions within the column.

As the intention of this experiment was to encourage the precipitation of Fe on the limestone particles, a process that requires O_2, initially the synthetic AMD was not purged with N_2 prior to the addition of $FeSO_4 \cdot 7H_2O$ and KCl. It was observed however, that the pH of the synthetic AMD within the carboy decreased during the course of the experiment, due to the oxidation of Fe(II) to Fe(III). To prevent this from occurring, the carboys containing the influent AMD were purged with N_2 to give an O_2 concentration of <1.5 mg/L. No oxidation was observed to take place within the carboys following this procedure (Fig. 2). In addition, the 500 mL flask in which the chemicals were dissolved was purged with N_2 prior to use. It should be noted that no precipitation occurred within the carboys during either procedure.

2.4. Sampling and analytical methods

Temperature and pH measurements of the influent and effluent solutions were recorded at 1–2-day

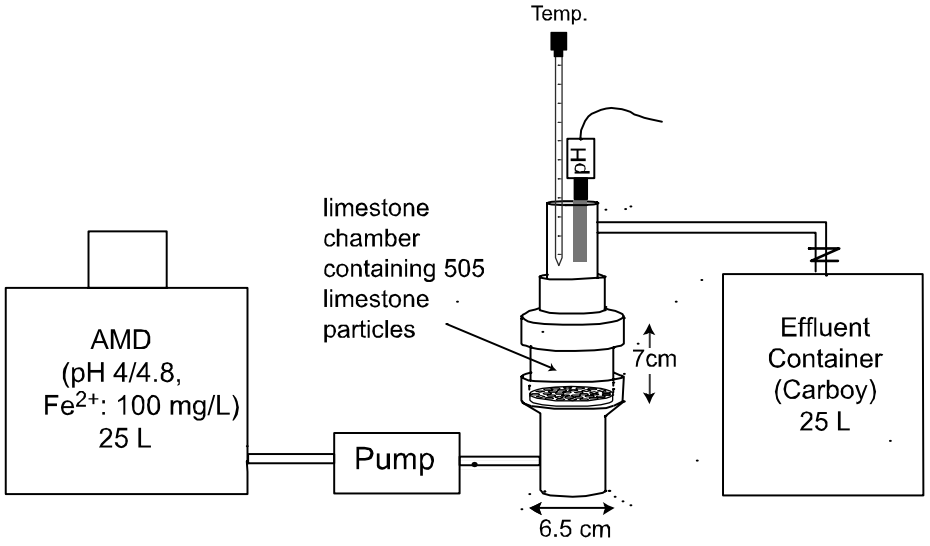

Fig. 1. Schematic diagram of laboratory setup. Not to scale.

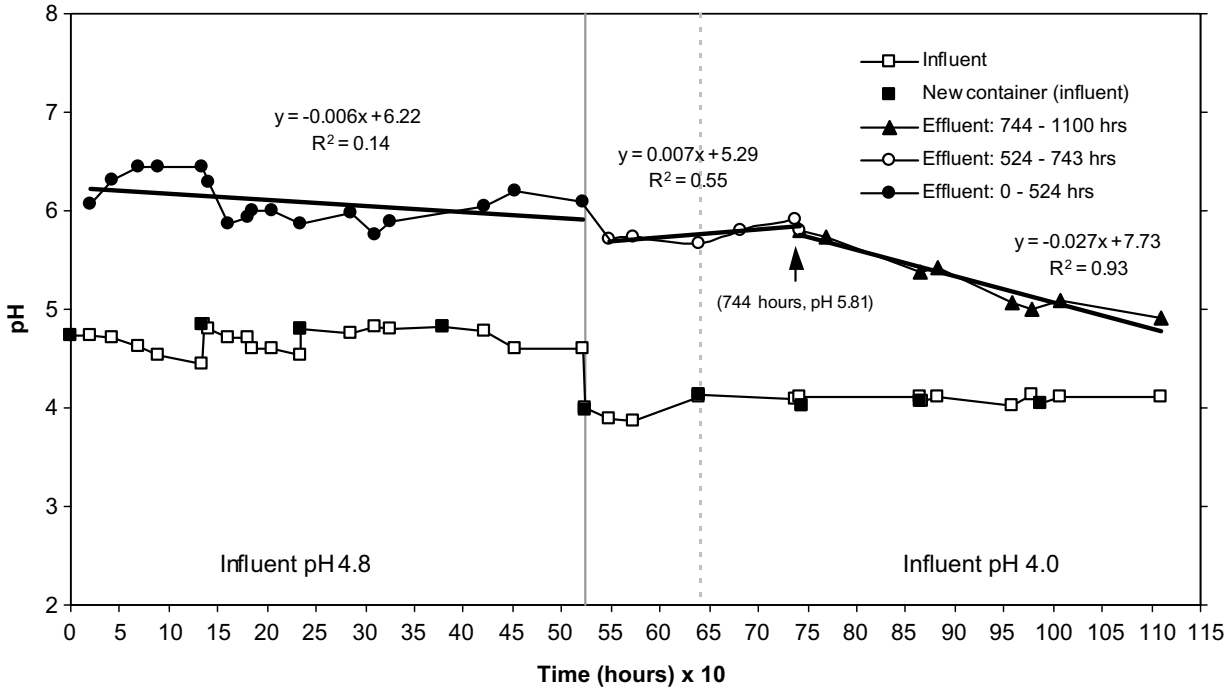

Fig. 2. Change in pH over time. The solid grey line indicates the point where the pH of the influent AMD was reduced from 4.8 to 4. The dashed line shows when experiment was suspended. Equations and correlation coefficients calculated for lines of best fit from either side of 744 h, when rate of pH decline increased (see text for discussion).

intervals during the 46-day experiment (see Fig. 1 for measurement locations). Neither the pH probe nor thermometer were fixed but were introduced to the experimental system when measurements were required. The pH probe was calibrated prior to each measurement. The experiment was temporarily suspended after 639 h for external reasons. During this time, the limestone system was filled with distilled water to prevent precipitation reactions from taking place.

Effluent water was collected in nine 25 L carboys (C1–C9). The contents in each carboy were thoroughly shaken, the volume measured using graduated cylinders, and one 150 mL sample taken in a polyethylene container that was completely filled. The pH and temperature of the effluent were measured using a Metrohm pH meter (Model 704) with the pH electrode initially calibrated using pH 4 and 6.86 buffer solutions. The 150 mL samples were not filtered but were acidified with 1.5 mL of concentrated HNO_3 and then refrigerated at 4 °C.

Concentrations of Fe, K, Mg and Ca in the effluent were determined by atomic absorption spectroscopy, and levels of Cl and SO_4 were measured using ion chromatography; the NO_3 peak did not interfere with analysis. Alkalinity levels were below detection limits in most samples (because of the low pH), and were determined by charge balance in the remainder. Activities of aqueous species and mineral saturation indices ($SI = \log(\text{activity product}/K_{eq})$) were calculated using PHREEQC Interactive v. 2.6 (Parkhurst and Appelo, 1999).

2.5. Characterisation of Fe hydroxide precipitates

At the conclusion of the experiment, the limestone grains, which were coated with Fe hydroxide precipitates, were removed from the column, air-dried for 4 weeks and weighed. The coatings on a random sample of limestone grains were removed using plastic tweezers, and examined under a Leica stereo light microscope to determine their texture and approximate thickness. The coating was composed of multiple layers (discussed in detail below) but could only be mechanically separated into two: a denser layer that was adjacent to the limestone surface and an overlying layer of loose Fe powder. The powdery layer was separated using a fine hair brush, crushed and analysed qualitatively for mineralogy using a Siemens D5000 X-ray diffractometer (XRD) and infra-red analysis (IR); similar analyses were performed on a bulk sample of the coating.

To determine the average thickness of the Fe coating on the limestone grains more accurately, and obtain an indication of the strength of bonding between the Fe coating and the limestone, samples were examined using a Cambridge S150 scanning electron microscope (SEM) operated at 20 kV with a Link AN10000 electron dispersive X-ray spectrometer (EDS). Coated limestone grains were arranged vertically in a 23 mm diameter nylon mould; the nylon mould was filled with a 1:4 solution of hardener/resin, allowed to set, and then cut. The cut surface was polished with carborundum followed by a 2 μm diamond wheel, and coated in a 120 nm layer of C before examination under the SEM.

2.6. Calculation of limestone surface area

To determine the thickness of the Fe encrustation around the limestone grains, it was necessary to know the total surface area of the 505 irregularly shaped limestone particles used in the experiment. Fifty limestone particles were randomly selected; the average surface area per unit mass of the 50 limestone grains was calculated from measurements of length and mass on each individual particle using the method of Pearson and McDonnell (1977):

$$\text{surface area/unit mass} = \frac{\frac{\pi D^2}{S}}{m} \tag{6}$$

where m is the mass of the limestone particle (g) and D is the nominal diameter (cm), equal to the diameter of a sphere of the same volume as the particle:

$$D = 2 \times \sqrt[3]{\frac{\text{vol}}{\frac{4}{3}\pi}} \tag{7}$$

where the particle volume is calculated from mass (g) × particle density (g/cm^3). Particle density was determined using the pycnometer method of McIntyre and Stirk (1954).

In Eq. (6), S is the shape factor of the particle, defined as the ratio of the surface area of a sphere with the same volume as the particle, to the surface area of the particle:

$$S = 1.15 - 0.25E \tag{8}$$

where elongation $(E) = L/D$; L is the maximum length of a particle and D the nominal diameter (calculated as above).

The values of surface area per unit mass of the 50 limestone grains were not normally distributed, exhibiting a positive skewness, and so the median rather than the mean was used as the average (Rees, 1985). The total surface area of the 505 limestone particles used in the experiment could then be calculated:

$$\text{Total surface area} = \text{median surface area /unit mass} \times \text{mass of 505 limestone particles} \tag{9}$$

2.7. Calculation of expected thickness of Fe coating on limestone grains

The expected thickness of the Fe encrustation around the limestone particles was calculated from the mass of Fe precipitated in the column, which is the difference between the total Fe content of the influent solution and that of the effluent. The mass of Fe precipitated was converted to a mass of Fe oxyhydroxide and then to a volume using an assumed density of 4.18 g/cm^3, which is the average density of goethite and lepidocrocite, the two minerals present in the Fe coating (see below). The volume of precipitate was then divided by the total mass of limestone particles used in the experiment (78.46 g) to derive the volume of Fe precipitated per gram of limestone. This was converted to a thickness around each particle by dividing by the average surface area per unit mass (calculated from Eq. (6)). The thickness of the Fe hydroxide coating calculated in this way was compared to the actual average thickness measured under the SEM.

3. Results and discussion

3.1. Limestone surface area

The limestone particles used in the experiment had a maximum length of 0.5–1.3 cm and a minimum length of 0.05–0.4 cm. The median surface area of the 50 limestone particles assessed was 0.9 cm^2, giving a median surface area per unit mass of 7.1 cm^2 g^{-1} and a total surface area of 560 cm^2 for the limestone particles in the column, which weighed 78.46 g.

3.2. Chemical trends

During the initial phase of the experiment, neutralisation within the limestone-filled column caused the influent pH (4.8) to increase to greater than 6 in

the effluent water, and the effluent pH reached a maximum of 6.45 after 68 h (Fig. 2). The influent water was acidic and highly undersaturated with respect to calcite, so the limestone in the column actively dissolved, as reflected in the high Ca and alkalinity concentrations in the effluent waters during the initial stage of the experiment (Table 1 and Fig. 3), when the rates of calcite dissolution and Fe precipitation were at their peak (Table 2 and Fig. 4). The maximum pH of 6.45 was maintained for 72 h after which it decreased gradually, falling to below 6 after 150 h. The decrease was probably due to the surfaces of the limestone particles becoming less reactive as they were progressively coated by Fe precipitates, as there was a concomitant reduction in the amount of Ca^{2+} in the effluent and therefore the rate of limestone dissolution (Figs. 3 and 4). The amount and rate of Fe precipitation also decreased (Figs. 3 and 4); because this reaction is partially driven by H^+ neutralisation (reaction (1)), as less limestone dissolves and the pH falls, less Fe will precipitate. As a result, it was decided to reduce the influent pH from 4.8. to 4 after 524 h (when 78.98 L of synthetic AMD had passed through the column), to increase the limestone dissolution within the system and hence encourage a greater precipitation of Fe.

Table 1
Composition of influent synthetic AMD and representative effluent waters (in mg/L except pH)

Sample	Average influent	Effluent (after 234 h; C2)	Effluent (after 1110 h; C9)
FE^{2+}	100.3	72.0	85.0
Ca^{2+}	0.0	39.9	12.2
Mg^{2+}	0.0	0.4	0.1
HCO_3^-	0.0	51.6	3.1
K^+	72.0	68.7	68.0
Cl^-	66.2	62.3	61.6
SO_4^{2-}	184	179	174
pH	4.24	5.99	4.90

The effluent pH showed an overall decline up to 500 h (−0.006 pH units/10 h; Fig. 2) with significant fluctuations, giving a poor correlation coefficient ($r^2 = 0.14$). The most likely cause of the fluctuations is variability in the influent pH due to differing degrees of oxidation of Fe(II) to Fe(III) within the carboys of synthetic AMD (reaction (3)). After 500 h, sparging with N_2 was used to remove O_2 from the influent solution, and no oxidation was observed to take place within the carboys for the remainder of the experiment; the effluent pH stabilised and greater correlation coefficients were observed (Fig. 2).

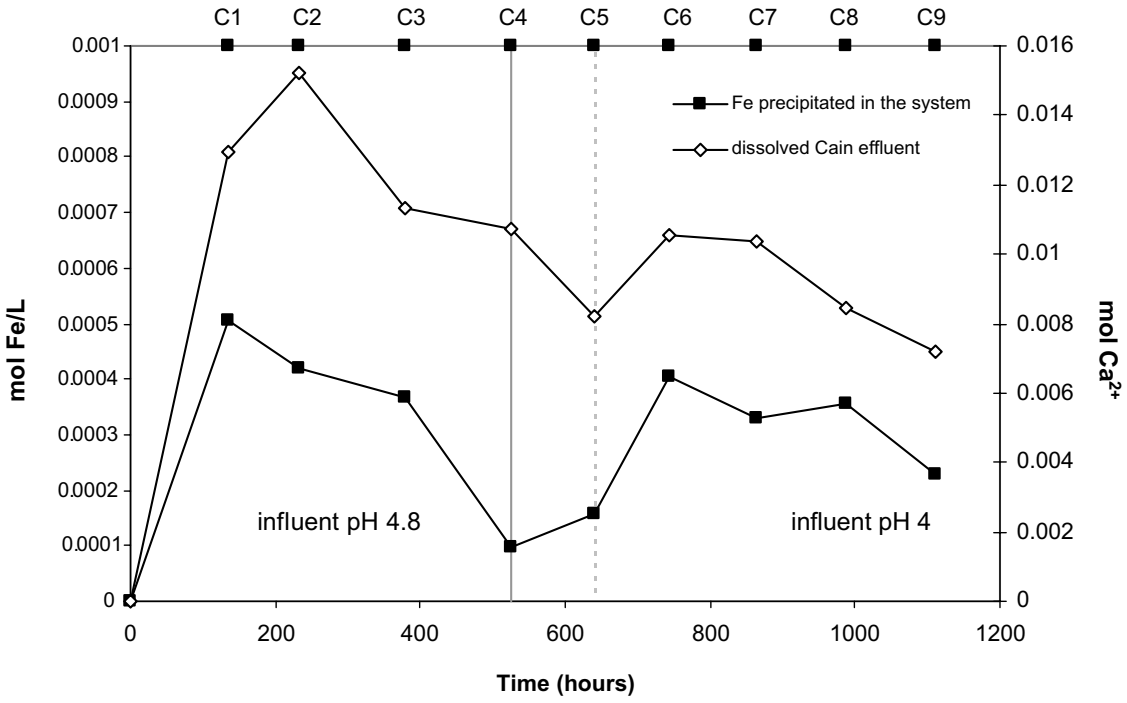

Fig. 3. Changes in amounts of Ca dissolved and Fe precipitated. Each tick mark on the top axis represents the time when a full container of effluent (C1–C9) was removed for analysis. The solid grey line indicates the point where the pH of the influent AMD was reduced from 4.8 to 4.

Table 2
Calculation of limestone dissolution and Fe precipitation rates from total amounts of Fe and Ca in effluent solutions

Effluent in carboy	Time (h)	Number of hours, *A*	Effluent volume (L), *B*	Influent Fe^{2+} concentration (mg/L)[a], *C*	Mass Fe introduced into column (g), *D*	Total Fe in effluent (g), *E*	Total Fe precipitated in column (g), *F*	Fe precipitated (%), *G*	Moles Ca^{2+} in effluent[b] ($\times 10^{-2}$), *H*	Mass $CaCO_3$ dissolved (g), *I*	Total mass of $CaCO_3$ in column at beginning of time period (g), *J*	Surface area (cm^2), *K*	$CaCO_3$ dissolution rate log (mmol cm^{-2} s^{-1}), *L*	Fe precipitation rate (mg Fe/h), *M*
C1	0–135	135	20.67	110.0	2.27	1.69	0.59	25.8	1.29	1.29	78.46	560	−7.32	4.35
C2	135–234	99	15.18	95.4	1.45	1.09	0.35	24.5	1.52	1.51	77.17	550	−7.11	3.58
C3	234–378	144	22.13	95.4	2.11	1.66	0.45	21.5	1.14	1.14	75.65	540	−7.39	3.15
C4	378–524	146	21.00	96.3	2.03	1.91	0.11	5.6	1.07	1.07	74.51	530	−7.41	0.77
C5	524–640	116	19.08	102.8	1.96	1.79	0.17	8.6	0.82	0.82	73.44	520	−7.42	1.47
C6	640–744	104	24.04	107.6	2.59	2.04	0.54	21.0	1.05	1.05	72.61	510	−7.26	5.20
Total to 744	Total to 744 h	744	122.10	Ave. 101.3	12.40	10.18	2.22	Ave. 17.9	6.89	6.89	71.59	510	−7.32	2.98
C7	744–865	121	23.69	97.1	2.3	1.87	0.44	19.0	1.03	1.03	71.56	510	−7.33	3.59
C8	865–988	123	23.50	100.7	2.37	1.90	0.47	19.8	0.84	0.84	70.53	500	−7.42	3.83
C9	988–1110	122	23.60	97.7	2.31	2.01	0.3	13.0	0.72	0.72	69.68	490	−7.48	2.45
Influent pH 4.8[c]	0–524	524.47	78.98	n/a	7.85	6.35	1.51	Ave. 19.3	5.02	5.03	78.46	Ave. 540	−7.31	2.87
Influent pH 4[d]	524–1110	585.27	113.90	n/a	11.52	9.61	1.92	Ave. 16.3	4.47	4.47	73.44	Ave. 510	−7.38	3.28
Total C1–C9	1110	1110	192.89	n/a	19.37	15.95	3.42	Ave. 17.7	9.49	9.49	78.46	560	−7.34	3.09

$D = ((C/55.85) \times 10^{-3})/B$; $F = D - E$; $G = (F/D) \times 100$; $I = H \times 100.09$ g/mol; $K = 7.077\ cm^2\ g^{-1} \times J$ (averages [Ave.], and not totals, are given where noted); $L = \log((H \times 1000)/(A \times K))$ where A is in s; $M = (F \times 1000)/(A)$.

[a] Calculated from the "catch-weight" of $FeSO_4 \cdot 7H_2O$.

[b] Equivalent to moles $CaCO_3$ dissolved.

[c] C1–C4.

[d] C5–C9.

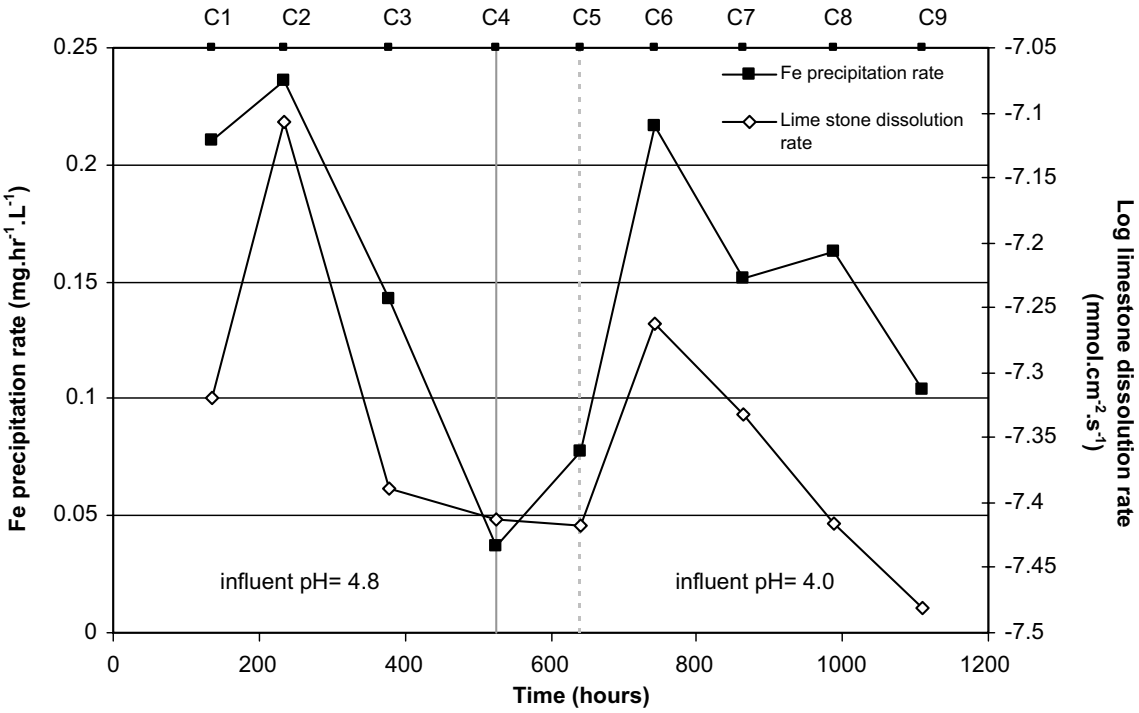

Fig. 4. Changes in the limestone dissolution and iron precipitation rates. Tick marks on the top axis indicate when full containers (C1–C9) were removed for analysis.

Following the reduction in influent pH to 4, the effluent pH increased slightly (0.007 pH units/10 h; $r^2 = 0.55$) until 744 h, when a noticeable change occurred (Fig. 2). The pH decline increased ~4 times to 0.027 pH units/10 h (the reason for this is discussed below), and remained at this rate until the experiment was terminated when the pH fell to 4.9, after 113.90 L of pH 4 synthetic AMD had passed through the system. The experiment was interrupted for external reasons at 639 h, but this had no effect on the rate of reaction (Fig. 2). During the course of the experiment, neutralisation of the AMD by the limestone was substantially hindered by the Fe precipitates coating the limestone particles, but nevertheless limestone dissolution continued to occur, as shown by the Ca released into solution (Fig. 3), albeit at a much slower rate after 744 h (Fig. 4), coinciding with a more rapid rate of effluent pH decrease (Fig. 2). Iron precipitation also continued to occur until the termination of the experiment, although a decrease in the Fe precipitation rate was observed after 744 h (Fig. 4), as the solution within the limestone column became less likely to precipitate Fe due to its lower pH (reaction (1)).

Concentrations of K^+ and Cl^- remained constant during the course of the experiment, indicating that there were no effects of evaporation or dilution. The levels of SO_4^{2-} also did not change (within experimental error), because concentrations of Ca^{2+} and SO_4^{2-} were too low for gypsum to precipitate (Fig. 5). XRD analysis confirmed that no gypsum was present in the coatings on the limestone grains.

3.3. Limestone dissolution

Limestone dissolved during the entire course of the experiment; the influent water was always undersaturated with respect to calcite (negative saturation indices; Fig. 5). During the first 744 h of the experiment, before the marked change in the rate of pH decline occurred, a total of 6.89 g of limestone dissolved (Table 2), representing a dissolution rate of $10^{-7.32}$ mmol cm^{-2} s^{-1}. In the later stages of the experiment (744 – 1110 h), the influent AMD was more acidic (pH 4), but the dissolution rate decreased to $10^{-7.38}$ mmol cm^{-2} s^{-1}. This reflects the reduced ability of the limestone to neutralise the AMD as Fe hydroxide coatings built up on the limestone particles. Despite the increased acidity of the water in the column, reflected in increasingly negative calcite saturation indices during the experiment (Fig. 5), the thickness of the coatings was sufficient to slow down limestone dissolution.

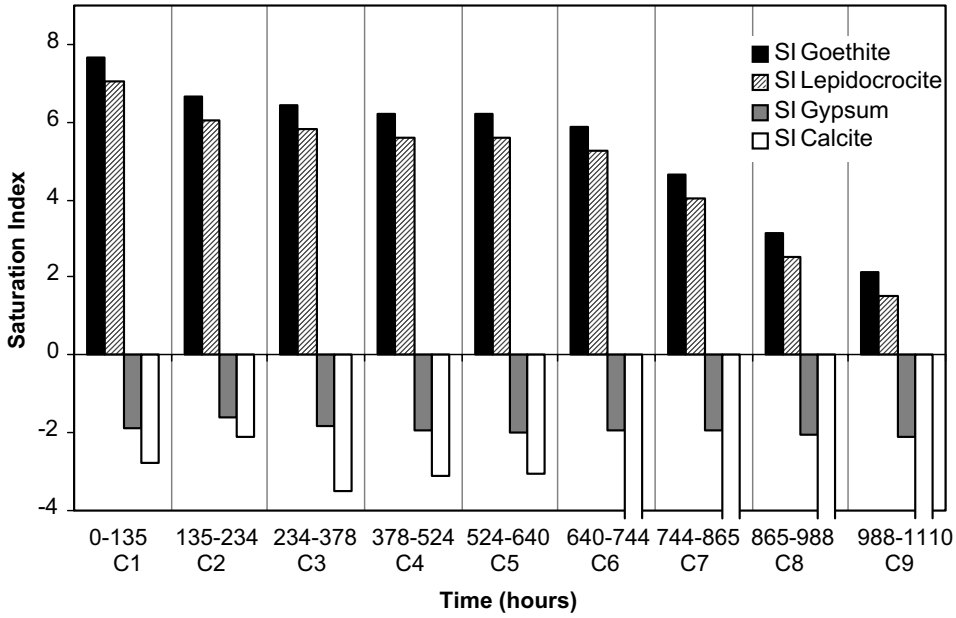

Fig. 5. Relative changes in saturation indices for goethite, lepidocrocite, gypsum and calcite during the experiment. SI indices for calcite and gypsum calculated using PHREEQC Interactive v. 2.6 (Parkhurst and Appelo, 1999). SI indices for goethite and lepidocrocite calculated using ΔG_f^0(goethite) = −486.87 kJ/mol ($\log K_{goethite} = 1.4$; Bigham et al., 1994) and ΔG_f^0(lepidocrocite) = −480.1 kJ/mol (after Majzlan et al., 2003); assuming pe of 4, i.e. moderately oxidising conditions (SI values for goethite and lepidocrocite may not be accurate but are consistent relative to each other, so trends of changes in SI are correct). Calcite saturation indices extend below −4 after 640 h.

The total mass of limestone dissolved during the course of the experiment (46.2 days), calculated from the Ca^{2+} concentrations in the effluent (Table 3), was 9.49 g, which is 12.1% of the total limestone in the column. This is in good agreement with the value of 9.48 g calculated from the difference between the initial (78.46 g) and final weights of limestone (68.98 g after subtracting the mass of Fe precipitated as determined from the water chemistry; Table 3).

The amount of limestone dissolved per unit surface area per unit time in the experiment is $10^{-7.38}$ mmol cm^{-2} s^{-1}. This is almost 4 times slower than the rate of $10^{-6.9}$ mmol cm^{-2} s^{-1} obtained by Cravotta and Trahan (1999) for the inflow portion of an open limestone drain in eastern USA. The influent pH in Cravotta and Trahan's (1999) experiment was lower (pH 3.5–4), so more limestone dissolved per unit surface area/s than in the present study. There were large differences in surface area between the two studies; Cravotta and Trahan (1999) used limestone slabs (1–2 cm thick by 3–4 cm wide) with a smaller surface area (~40 cm^2) than in the present experiment (560 cm^2), resulting in a much lower surface area/g limestone in their study (1 cm^2 g^{-1} compared to 7 cm^2 g^{-1}). As a result, approximately twice as much limestone dissolved/g of limestone in this study (1 g g^{-1} a^{-1}) than in Cravotta and Trahan's (1999) experiments (0.43 g g^{-1} a^{-1}).

Table 3
Calculation of amounts of Fe hydroxide precipitation and limestone dissolution

A	Total mass of Fe in influent AMD[a]	19.37 g
B	Total mass of Fe in effluent[a]	15.95 g
C	Total mass of Fe retained in column	3.42 g
D	Total mass of FeOOH retained in column[b]	5.45 g
E	Total mass of FeOOH precipitated on limestone	5.24 g
F	Initial mass of limestone	78.46 g
G	Final mass of limestone and FeOOH coatings	74.22 g
H	Final mass of limestone	68.98 g
I	Amount of limestone dissolved	9.48 g

$C = A - B$; $E = D$ – mass (FeOOH) retained on column walls (0.21 g); $H = G - E$; $I = F - H$.
[a] From Table 2.
[b] Conversion of C from Fe to FeOOH using molar mass ratio (1:1.59).

3.4. Iron precipitation

In total, 19.37 g of Fe passed through the column in 192.89 L of synthetic AMD containing on average 100.3 mg/L Fe^{2+}; 17.7% of the Fe was retained in the column (Table 2) by precipitation, which occurred during the entire course of the experiment (Fig. 3) at an average rate of 3.09 mg/h (Table 2). The greatest rate of precipitation occurred after 640 h when the influent pH was reduced to 4.

The percentage of Fe precipitated in the experiment (17.7%) is comparable to results from anoxic limestone drains in eastern USA (median 28%; Fig. 6), but is lower than expected for oxic limestone systems, where Fe precipitation can reach almost 100% (Cravotta and Trahan, 1999). In the experiment O_2 levels in the influent solution were low, as the synthetic AMD was sparged with N_2 to <1.5 ppm O_2, and the configuration of the column (Fig. 1) prevented significant O_2 infiltration and hence metal precipitation, whereas in oxic limestone drains, influent solutions contain relatively high O_2 concentrations (in equilibrium with the atmosphere), which promote metal precipitation. In general, the Fe retention within limestone drains is dependant primarily upon O_2 concentrations within the system, and is little affected by influent Fe concentration or influent pH (Fig. 5).

The Fe hydroxide minerals in the coatings on the limestone grains are goethite (α-FeOOH) and lepidocrocite (γ-FeOOH), as identified by XRD and IR analysis (discussed further below). Saturation indices (SI) show that the effluent was supersaturated (SI > 0) with respect to these minerals during the full course of the experiment (Fig. 5). The free energies of formation (ΔG) of goethite and lepidocrocite differ by less than 10 kJ/mol (Bigham et al., 1994; Majzlan et al., 2003), so their saturation indices are always similar.

The dissolution reaction for goethite and lepidocrocite:

$$\mathrm{FeOOH(s)} + 3\mathrm{H^+} = \mathrm{Fe^{3+}} + 2\mathrm{H_2O} \quad (10)$$

means that their saturation indices are inversely proportional to the log of activity of H^+:

$$\mathrm{SI_{goe./lep.}} = \log \frac{\frac{a\mathrm{Fe^{3+}}}{(a\mathrm{H^+})^3}}{K_{\mathrm{eq}}} \quad (11)$$

Therefore, as pH decreased (and log$a$H$^+$ increased) during the experiment, the saturation indices for goethite and lepidocrocite decreased (Fig. 5); the rate of decline in both pH and the saturation indices was greatest after 744 h (the reason for this is discussed below).

Up until 744 h, when the limestone dissolution and Fe precipitation rates decreased, a total of 3.53 g of FeOOH (2.22 g as Fe) had precipitated within the column at a rate of 2.98 mg/h (Table 2). During the entire course of the experiment, a total of 5.45 g of FeOOH (3.42 g as Fe) was retained within the column (Table 2). Of this, 0.21 g FeOOH (0.13 g as Fe) adhered to the sides of the column (obtained from the difference in air-dry weight of the column before and after the experiment), so 5.24 g FeOOH (3.30 g as Fe) precipitated on the limestone grains (Table 3). The amount of FeOOH that precipitated on the sides of the column up until 744 h, assuming that it is proportional to the overall rate of Fe precipitation, was 0.13 g of FeOOH (0.08 g as Fe), so 2.14 g of Fe precipitated on the surface of the limestone particles up until this time.

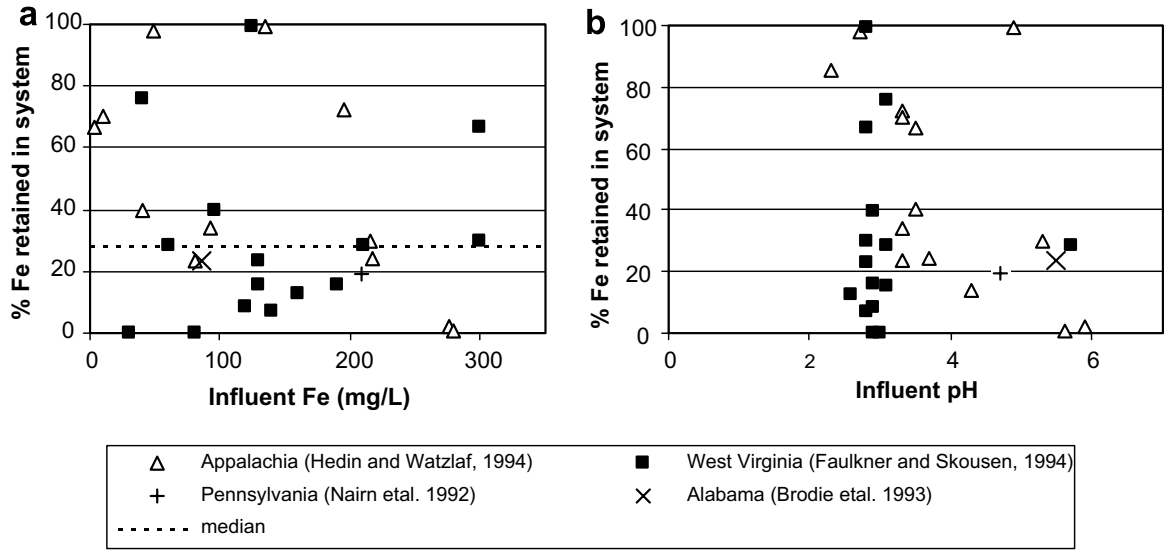

Fig. 6. Percentage of Fe retained in anoxic limestone drains from different locations in eastern USA as a function of influent metal concentration (a) and influent pH (b). Data exhibiting negative % Fe retained are not included. Dotted line indicates the median % Fe retained (28%).

3.5. Iron hydroxide precipitates

Iron hydroxide covered more than 95% of the surface of the limestone grains; coatings were thin or absent where the particles contacted one another. Three distinct layers are present: a thick porous orange layer adjacent to the surface of the limestone (Layer 1), overlain by a dark brown non-porous crust (Layer 2), succeeded by a powdery layer of loosely-bound, porous orange globules (Layer 3) (Fig. 7a). SEM imagery indicates that the density of Layer 1 increases away from the limestone surface (Fig. 7b). This sequence was also recorded by Clarke et al. (1985), who precipitated Fe hydroxides from a $Fe(ClO_4)_2$ solution relatively rapidly (days rather than weeks). However, Clarke et al. (1985) did not observe the ~60 μm wide void space between the limestone and Fe hydroxide layers (Fig. 7b).

The thick porous Fe hydroxide layer (Layer 1) represents the first phase of Fe precipitation. Initially the large reactive surface area of the limestone grains allowed rapid neutralisation of the influent acidity, and a boundary layer of solution depleted in H^+ built up around the limestone grains. The products of the limestone neutralisation, HCO_3^- and/or H_2CO_3 (reactions (4) and (5)), could diffuse rapidly into the surrounding solution at this stage of the experiment. Removal of H^+ favours Fe hydroxide precipitation (reaction (1)); as a consequence, a relatively thick band of porous Fe hydroxide formed from rapid precipitation at the outer edge of the H^+-depleted boundary layer, a finite distance from the limestone grain. During the earlier stages of the experiment when the Fe coating was relatively thin and porous, it is likely that the presence of this void space meant that the rate of limestone dissolution was little affected; Cravotta et al. (2004) proposed that thinly coated and uncoated limestone dissolve at comparable rates.

The overlying dense crust probably represents a period of slower growth, attributed by Clarke et al. (1985) to a diffusion barrier formed by the growing Fe hydroxide coating, slowing the movement of Fe^{3+}/Fe^{2+} and H^+ towards the calcite surface. By also reducing the rate of diffusion of H_2CO_3

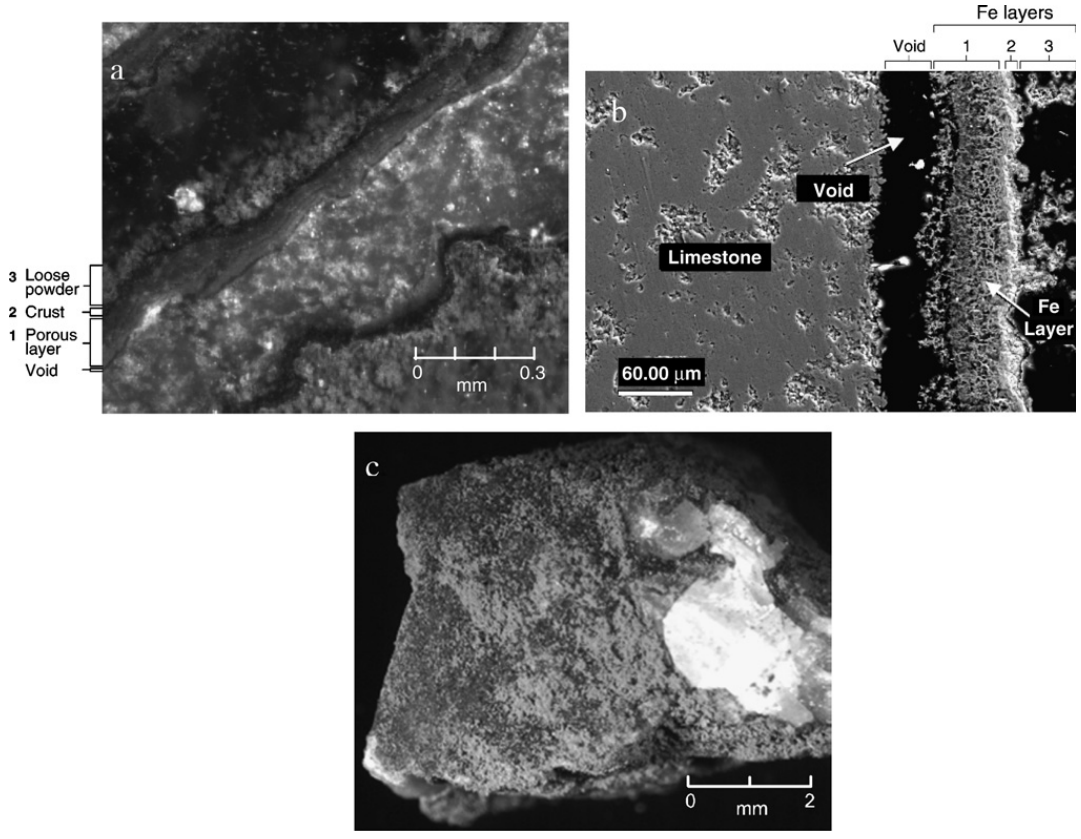

Fig. 7. Photomicrographs of (a) cross-section of Fe hydroxide coating on a limestone particle, showing layers present; (b) SEM image showing the void space between the limestone and Fe layers; (c) limestone particle with portion of crust removed revealing unstained limestone beneath.

away from the surface of the limestone, the barrier could locally elevate H_2CO_3 concentrations and potentially cause further limestone dissolution (Cravotta et al., 2004):

$$CaCO_3 + H_2CO_3^0 \rightarrow Ca^{2+} + 2HCO_3^- \quad (12)$$

Once the dense crust encapsulated the limestone grains, neutralisation of the influent AMD by the limestone would have been severely impeded (but not completely stopped). This presumably occurred at 744 h through the experiment, when pH (and the saturation indices of goethite and lepidocrocite) began to decline more rapidly (Fig. 5). Thus, formation of the crust was responsible for the ultimate failure of the system.

Above the dense crust is a powdery layer of loosely-bound, porous orange globules that probably represent settling of suspended grains of Fe hydroxide that precipitated in the solution above the limestone surface (Clarke et al., 1985).

The complete Fe hydroxide coating required minimal force to be completely removed from the limestone surface, reflecting the observed void between the two, and fragmented easily (like the shell of a hard-boiled egg). There was little orange/yellow staining on the limestone after the coating was removed (Fig. 7c), and SEM analysis showed no transitional region between the two materials. Thus, the Fe hydroxide coating was not adhesively bound to the surface of the limestone, although the layers within the coating cannot be separated. Loosely bound amorphous to crystalline Fe hydroxide/Fe–Al hydroxysulfate coatings have been observed to precipitate on limestone grains in a number of studies, precipitated in both laboratory and field situations and from AMD and $Fe(ClO_4)_2$/$Fe(ClO_4)_3$ solutions (Leoppert and Hossner, 1984; Hammarstrom et al., 2003; Cravotta and Watzlaf, 2002; Huminicki and Rimstidt, 2004). However, Schwertmann and Friedl (1998) noted very strongly adherent goethite and ferrihydrite films on limestone and other pebbles in AMD streams, and experiments by Scheidegger et al. (1993) produced strongly bonded goethite coatings on quartz grains, attributed to the formation of Fe–O–Si bonds. The mineralogy of both the Fe hydroxide coatings and the grains to which they are bound may influence the strength of adhesion of the coatings.

XRD and IR analysis showed that all layers of the Fe hydroxide coatings in the present experiment are composed of a mixture of goethite and lepidocrocite (Figs. 8 and 9), and the IR spectra indicate that ferrihydrite is absent. The half peak heights of all XRD spectra are similar, indicating that the different layers have the same crystallinity.

In the present experiment it is not possible to say with certainty whether goethite and lepidocrocite are primary precipitates or have replaced ferrihydrite, which precipitated first. However, the formation of primary goethite and lepidocrocite at AMD sites has been widely reported (Karathanasis and Thompson, 1995; Kim and Kim, 2003; Kirby et al., 1999). The precipitation of ferrihydrite is kinetically favoured, but lepidocrocite rather than ferrihydrite will form directly from Fe^{2+} solutions when oxidation is slow, pH is 5–7.5 (Cornell and Schwertmann, 2003), and/or Cl^- is present (Schwertmann and Taylor, 1972). In addition, crystalline rather than amorphous Fe hydroxide minerals form during limestone neutralisation of AMD when precipitation is slow (Clarke et al., 1985).

Lepidocrocite is metastable relative to goethite, and transformation to goethite is promoted by SO_4^{2-} (Carlson and Schwertmann, 1990) and the presence of Fe^{2+} (Cornell and Schwertmann, 2003). In this study, the high SO_4^{2-} and Fe^{2+} content of the synthetic AMD (Table 1) probably helped the partial recrystallisation of lepidocrocite to goethite.

The average thickness of the Fe hydroxide coatings around the limestone particles when the experiment was terminated can be calculated from the weight of goethite/lepidocrocite precipitated (5.24 g; Table 3), converted to a volume (1.25 cm^3) using a density of 4.18 g/cm^3 (average of densities of lepidocrocite [4.09 g/cm^3] and goethite [4.26 g/cm^3]). The total surface area of the limestone particles was 560 cm^2, so the calculated average thickness of the Fe hydroxide coating is 23 μm. After 744 h, when the rate of neutralisation decreased markedly and the system began to fail, the amount of FeOOH that had precipitated on the limestone was 3.53 g, giving a calculated coating thickness at this stage of the experiment of 15 μm. Both figures are underestimates, as they are based on the incorrect assumptions that the coating is non-porous and uniformly and evenly distributed. Nevertheless, they represent useful minimum values.

The average thickness of the FeOOH coating measured under the SEM is 80 μm (from 20 randomly selected limestone particles). As expected, this is higher than the calculated thickness (23 μm), due largely to the porosity of the coating. The orange porous layer is thicker (median 60 μm) than the overlying dense crust (median 20 μm).

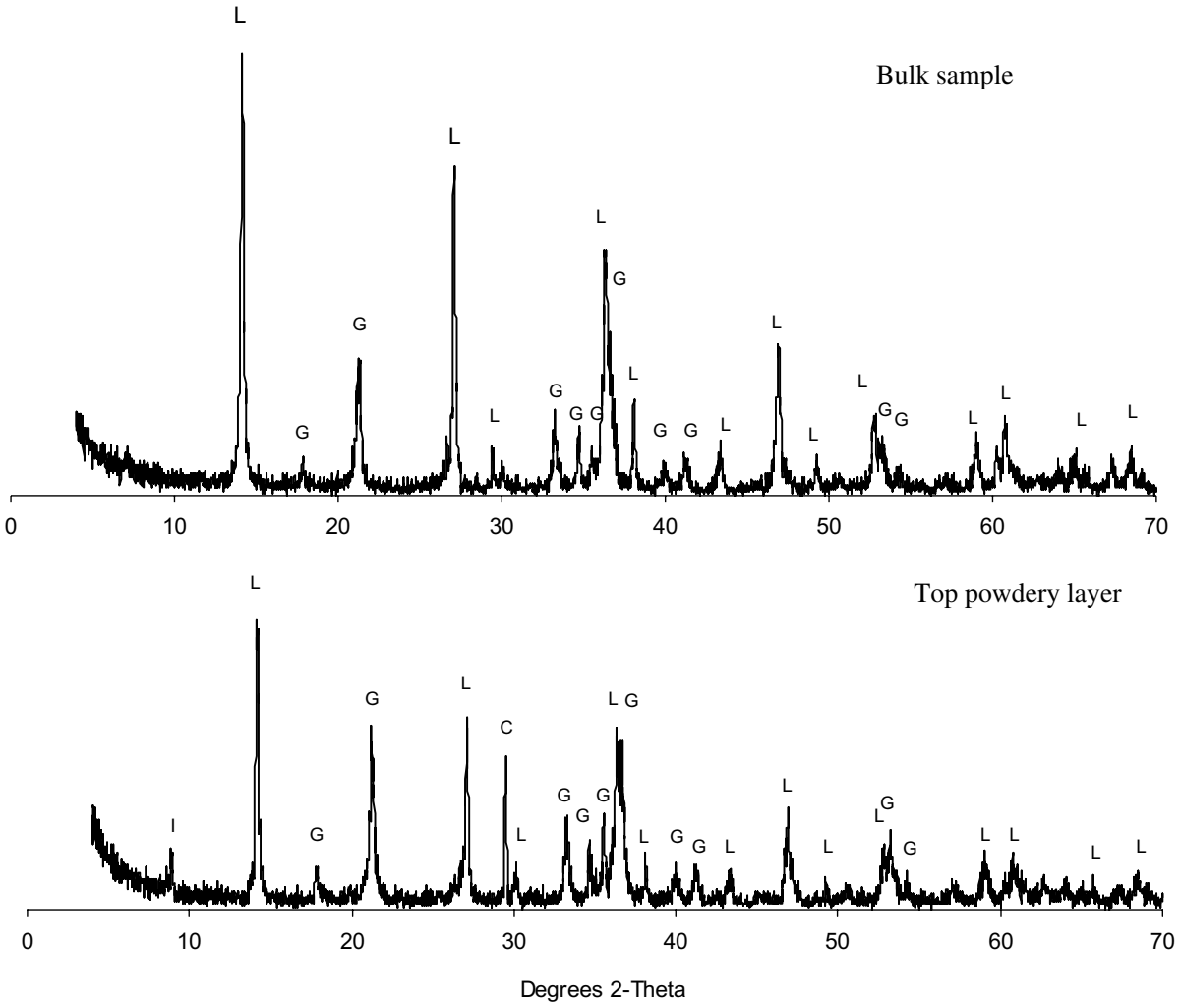

Fig. 8. X-ray powder diffractograms of Fe hydroxide coating (bulk sample and top powdery layer). L = lepidocrocite; G = goethite; I = illite; C = calcite.

The void between the limestone and hydroxide coating was 60 μm wide, but this may be a slight overestimate, as intrusion of epoxy resin during sample preparation could have enlarged the void.

3.6. Longevity of limestone drains

Previous studies on the longevity of limestone drains have focussed on the rates of limestone dissolution and alkalinity generation, and have not specifically considered the role of Fe precipitates in shortening the lifetime of the system. Hedin and Watzlaf (1994) evaluated alkalinity generation and limestone dissolution rates for 21 limestone drains to determine the optimum limestone properties for maximum alkalinity production, and derived a linear decay equation for limestone dissolution. Cubitainer tests by Cravotta and Watzlaf (2002) indicated that the behaviour should be exponential rather than linear, and provided good estimates for the long-term trends observed at three limestone drain sites.

In this study it has been shown that the limestone dissolution rate is severely affected by the formation of Fe precipitates on the limestone grains, such that when high levels of Fe^{2+} and sufficient O_2 are present in the influent AMD or treatment system, Fe hydroxide precipitation is the determining variable for the longevity of the system. When the AMD contains little Fe and/or O_2 (and Al is not present in significant concentrations), limestone dissolution and alkalinity generation rates control the lifetime of the limestone drain.

This study also demonstrated that there is a well-defined point in time when the Fe precipitate coating the limestone grains significantly decreases the AMD neutralisation, such that a marked increase in the rate of pH decline occurs (Fig. 1). This prob-

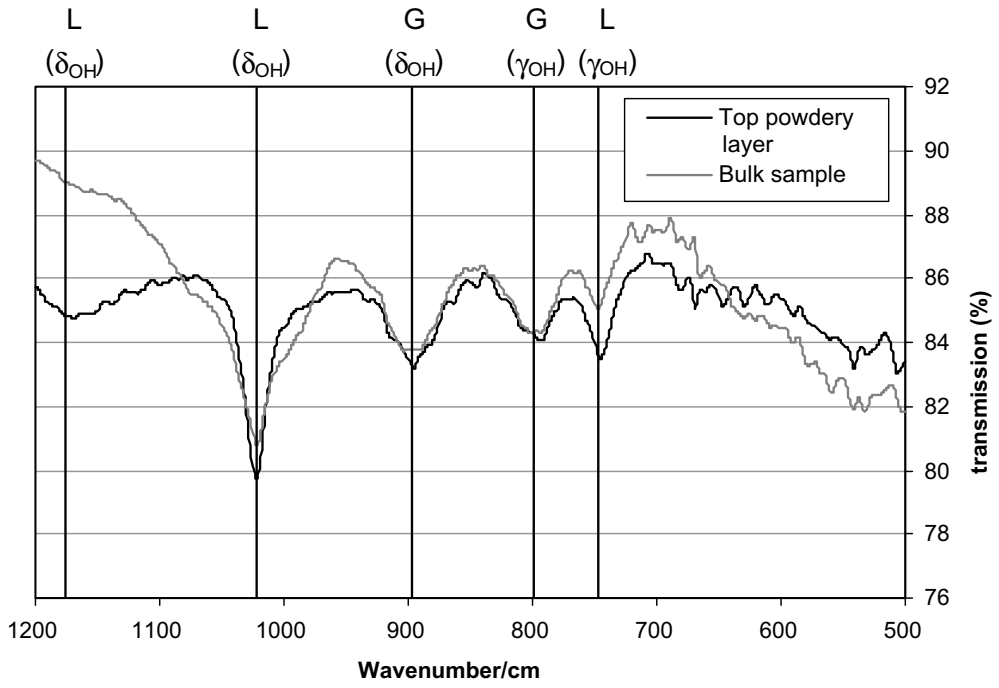

Fig. 9. Infra-red spectra of Fe hydroxide coating (bulk sample and top powdery layer) in the range 500–1200 cm^{-1}. G = goethite; L = lepidocrocite.

ably represents the time when the dense crust within the coating (Fig. 7) effectively encapsulated the exposed surfaces of limestone grains, severely impeding neutralisation. Thus, formation of the crust was responsible for the reduction in effectiveness and eventual failure of the system. In the present experiment, this occurred after 744 h, when 18% of Fe that had passed through the column had precipitated on the limestone grains. In field situations, the limestone within an oxic or anoxic limestone drain would need to be replaced at this stage, mechanically agitated or flushed to dislodge the precipitates, so that efficient neutralisation could continue to take place.

From the present study, the system began to exhibit the distinct decline in the rate of neutralisation when the total mass of Fe hydroxide precipitate (2.14×10^4 mg) was 3.85×10^4 times the total surface area of the limestone particles (5.60×10^{-2} m^2), i.e.:

$$\text{mass of Fe hydroxide precipitate (mg)} = \text{surface area } (m^2) \times 38{,}500 \quad (13)$$

The time taken for this amount of Fe to precipitate will be determined by the Fe^{2+}concentration in the influent AMD, the flow rate through the system, and the proportion of Fe within the influent AMD that is oxidised to Fe^{3+} and retained in the system as a precipitate. Incorporating the above factor (38,500) derived from this study gives the following relationship for the time when an anoxic limestone drain will begin to fail, where the factor initially derived (38,500) has been corrected for converting flow rate from hours to years:

$$t \text{ (years)} = \frac{\text{surface area } (m^2) \times 4.4}{\text{fraction Fe retained in system} \times [Fe^{2+}] \text{ (mg/L)} \times \text{flowrate (L/h)}} \quad (14)$$

Eq. (14) is directly applicable to anoxic limestone drains, which were duplicated by the experimental system in this study, and can also be used for oxic drains and open limestone channels, which will be characterised by much higher fractions of Fe retained in the system. The relationship derived assesses the longevity of these passive treatment systems in field situations, by indicating the time when the limestone needs to be either replaced or mechanically agitated to remove the Fe hydroxide coating,

to maintain high rates of AMD neutralisation. For mechanical agitation to be effective in prolonging the life of a limestone drain, the Fe hydroxide coating on the limestone grains must be easily removed, as in the present experiment, where a 60 μm void separated the coating from the limestone. Agitation could fail if the precipitates are strongly adherent. Various systems have been designed to agitate the limestone in a passive system and flush out any solids dislodged, e.g. using a network of perforated pipes buried in the limestone (Vinci and Schmidt, 2001; Schueck et al., 2004); Weaver et al. (2004) reviewed these flushing technologies.

Eq. (14) can be tested by applying it to some documented passive limestone treatment systems. In the oxic limestone drain described by Cravotta and Trahan (1999), 1.37 mg/L Fe is present in the influent AMD and >99% of Fe is retained in the drain, so the time when the rate of neutralisation would begin to decrease is 8.3 a. Two anoxic limestone drains in Alabama (Brodie et al., 1993) and Pennsylvania (Nairn et al., 1992) have, respectively, substantially higher Fe concentrations of 65 and 208 mg/L, Fe retentions of 23.5% and 19.2% and flow rates of 128 and 7.5 L/min, giving calculated times for the drop in neutralisation rate of 1.7 and 1.4 a, respectively. For an anoxic limestone drain in Tennessee (Brodie et al., 1993), where the influent Fe concentration is 170 mg/L and flow rate is 1544 L/min, the estimated time for failure is 175 days, assuming an Fe retention of 28% (based on average Fe precipitation rates observed for other anoxic limestone systems; Fig. 6).

Therefore, even at moderately high influent Fe concentrations, most passive limestone systems will retain their maximum neutralisation potential for one to several years before they begin to fail. Thus, the recommendations that these systems should be used only if the Fe^{3+} level in the AMD is less than 1 and 10–20 mg/L for anoxic and oxic limestone drains, respectively (Hedin et al., 1994; Sterner et al., 1998) are too stringent. In addition, the results of the present study indicate that the Fe precipitates armouring the limestone grains may be loosely bound and relatively easily dislodged and flushed from the limestone bed, increasing the potential longevity of the passive limestone system. Therefore, limestone drains are more widely applicable than presently realised.

4. Conclusions

This study used a small-scale laboratory anoxic limestone drain to study how precipitation of Fe hydroxide affects the system's neutralising potential. From the results of the experiment, the following conclusions can be drawn:

1. Where passive limestone systems have been implemented to treat acid mine drainage containing significant levels of Fe, the longevity of a system will be determined by the amount of Fe hydroxide precipitate on the limestone grains rather than the rates of limestone dissolution and alkalinity generation.
2. There is a well-defined point in time when the Fe precipitate coating the limestone grains significantly decreases the AMD neutralisation, such that a marked increase in the rate of pH decline occurs. This represents the time when the system has begun to fail.
3. The Fe hydroxide coating is composed of lepidocrocite/goethite in three distinct layers: an initial thick porous orange layer (median thickness 60 μm), overlain by a dense dark brown crust (median thickness 20 μm), succeeded by a layer of loosely-bound, porous orange globules. When the dense crust effectively encapsulates the limestone grains, it severely impedes neutralisation and is responsible for the decline in the rate of limestone dissolution and the effective failure of the system.
4. A 60 μm wide void separates the limestone and the coating, so the precipitate could be easily removed from the limestone by agitation, allowing the limestone system to resume functioning at its maximum potential.
5. The experimental system began to fail when the total mass of Fe hydroxide precipitate was 3.85×10^4 times the total surface area of the limestone particles. Using this factor the following general relationship can be derived for the time taken for an anoxic limestone drain to start to fail:

$$t\ (\text{years}) = \frac{\text{surface area } (\text{m}^2) \times 4.4}{\text{fraction Fe retained in system} \times [\text{Fe}^{2+}]\ (\text{mg/L}) \times \text{flowrate } (\text{L/h})}.$$

At this time the limestone in the drain would need to be replaced or mechanically agitated to remove the Fe hydroxide coating, to maintain a high rate of AMD neutralisation.

6. Application of this formula shows that limestone drains described in the literature will function at their maximum neutralising capacity for one to several years before they begin to fail, even when the influent Fe concentrations are moderately high. Thus, recommendations that passive limestone systems should be used only if the Fe level in the AMD is less than 1–20 mg/L are too stringent, particularly given that the Fe precipitates armouring the limestone grains may be loosely bound and relatively easily dislodged, increasing the longevity of the system. Therefore, limestone drains are more widely applicable than presently realised.

Acknowledgements

Limestone was obtained from David Mitchell Ltd. The authors thank Dr. Rob Glaisher for conducting SEM analysis, and Terry Ryan and Alan Jacka for assistance with the design and construction of the laboratory apparatus. Chuck Cravotta, J. Hammarstrom and an anonymous referee provided helpful comments that substantially improved this paper. The study was partially funded by the AusIMM Bicentennial Gold Endowment 88.

References

Arnold, D.E., 1991. Diversion wells – a low-cost approach to treatment of acid mine drainage. In: Proceedings of the 12th West Virginia Surface Mine Drainage Task Force Symposium, Morgantown, WV, pp. 10–15.

Bigham, J.M., Carlson, L., Murad, E., 1994. Schwertmannite, a new oxyhydoxysulfate from Pyhasalmi, Finland, and other localities. Mineral. Mag. 58, 641–648.

Brodie, G.A., Britt, C.R., Tomaszewski, T.M., Taylor, H.N., 1993. Anoxic limestone drains to enhance performance of aerobic acid drainage treatment wetlands: experiences of the Tennessee Valley Authority. In: Moshiri, G.A. (Ed.), Constructed Wetlands for Water Quality Improvement. Lewis Publ., Boca Raton, FL, pp. 129–138.

Carlson, L., Schwertmann, U., 1990. The effect of CO_2 and oxidation rate on the formation of geothite versus lepidocrocite from an Fe(II) system at pH 6 and pH 7. Clay Min. 25, 1712–1719.

Clarke, E.T., Loeppert, R.H., Ehrman, J.M., 1985. Crystallization of iron oxides on calcite surfaces in static systems. Clay Clay Min. 33, 152–158.

Cornell, R.M., Schwertmann, U., 2003. The Iron Oxides. Structure, Properties, Reactions, Occurrences and Uses. Wiley–VCH GmbH & Co., KGaA, Weinheim.

Cravotta, C.A., Trahan, M., 1999. Limestone drains to increase pH and remove dissolved metals from acidic mine drainage. Appl. Geochem. 14, 581–606.

Cravotta, C.A., Watzlaf, G.R., 2002. Design and performance of limestone drains to increase pH and remove metals from acidic mine drainage. In: Naftz, D., Morrison, S.J., Fuller, C.C., Davis, J.A. (Eds.), Handbook of Groundwater Remediation Using Permeable Reactive Barriers – Applications to Radionuclides, Trace Metals, and Nutrients. Academic Press, San Diego, CA, pp. 19–66 (Chapter 12).

Cravotta, C.A., Ward, S.J., Koury, D.J., Koch, R.D., 2004. Optimization of limestone drains for long-term treatment of mine drainage, Swatara Creek Basin, Schuylkill County, PA, 2004. In: National Meeting of the American Society of Mining and Reclamation and the 25th West Virginia Surface Mine Drainage Task Force, ASMR, Lexington, KY, pp. 366–410.

Faulkner, B.B., Skousen, J., 1995. Effects of land reclamation and passive treatment systems on improving water quality. Green Lands 25, 34–40.

Garrels, R.M., Christ, C.L., 1965. Solutions, Minerals and Equilibria. Harper & Row, NY.

Hammarstrom, J.M., Sibrell, P.L., Belkin, H.E., 2003. Characterisation of limestone reacted with acid-mine drainage in a pulsed limestone bed treatment system at the Friendship Hill National Historical Site, Pennsylvania, USA. Appl. Geochem. 18, 1705–1721.

Hedin, R.S., Watzlaf, G.R., 1994. The effects of anoxic limestone drains on mine water chemistry. In: Proceedings of the International Land Reclamation and Mine Drainage Conference Third International Conference Abatement of Acidic Drainage, pp. 185–194.

Hedin, S.R., Nairn, R.W., Kleinmann, R.L.P., 1994. Passive treatment of Coal Mine Drainage. Bureau of Mine Information Circular, no. 9389.

Huminicki, D.M.C., Rimstidt, J.D., 2004. The effect of secondary precipitates on the dissolution rate of calcite in AMD solutions. In: Wanty, R.B., Seal, R.R.I. (Eds.), Proceedings of the 11th International Symposium on Water Rock Interaction, WRI 11, Balkema, Rotterdam, pp. 1531–1534.

Karathanasis, A.D., Thompson, Y.L., 1995. Mineralogy of iron precipitates in a constructed acid mine drainage wetland. Soil Sci. Soc. Am. J. 59, 1773–1781.

Kepler, D.A., McCleary, E.C., 1994. Successive alkalinity-producing systems (SAPS) for the treatment of acidic mine drainage. In: International Land Reclamation and Mine Drainage Conference U.S. Bureau of Mines SP 06A-94, Pittsburgh, PA, pp. 195–204.

Kim, J.J., Kim, S.J., 2003. Environmental, mineralogical, and genetic characterization of ochreous and white precipitates from acid mine drainages in Taebaeg, Korea. Environ. Sci. Technol. 37, 2120–2126.

Kirby, C.S., Decker, S.M., Macander, N.K., 1999. Comparison of color, chemical and mineralogical compositions of mine drainage sediments to pigment. Environ. Geol. (Berl.) 37, 243–254.

Leoppert, R.H., Hossner, L.R., 1984. Reactions of Fe^{2+} and Fe^{3+} with calcite. Clay Clay Min. 32, 213–222.

Majzlan, J., Grevel, K., Navrotsky, A., 2003. Thermodynamics of Fe oxides: Part II. Enthalpies of formation and relative stability of goethite (a-FeOOH), lepidocrocite (g-FeOOH), and maghemite (g-Fe_2O_3). Am. Mineral. 88, 855–859.

McDonald, D., Webb, J.A., 2005. Prediction of sludge composition and water quality from lime neutralisation of acid rock drainage (ARD). In: Proceedings of the Fifth Australian Workshop on Acid Drainage, Fremantle, Australia.

McIntyre, D.S., Stirk, K.B., 1954. A method for determination of apparent density of soil aggregates. Aust. J. Agric. Res. 5, 291–296.

Nairn, R.W., Hedin, R.S., Watzlaf, G.R., 1991. Preliminary review of the use of anoxic limestone drains in the passive treatment of acid mine drainage. In: Proceedings of the 12th West Virginia Surface Mine Drainage Task Force Symposium, Morgantown, WV, pp. 1–15.

Nairn, R.W., Hedin, R.S., Watzlaf, G.R., 1992. Generation of alkalinity in an anoxic limestone drain. In: Proceedings of the Ninth Annual National Meeting of the American Society for Surface Mining and Reclamation, Duluth, Minnesota, pp. 206–219.

Parkhurst, D.L., Appelo, C.A.J., 1999. User's guide to PHREEQC (Version 2) – a computer program for speciation, batch-reaction, one-dimensional transport, and inverse geochemical calculations. U.S. Geol. Surv. Water-Resour. Invest. Rep., 99-4259.

Pearson, F.H., McDonnell, A.J., 1975. Use of crushed limestone to neutralise acid wastes. J. Environ. Eng. Div. 101 (EE1), 139–158.

Pearson, F.H., McDonnell, A.J., 1977. Characterization of coarse porous media. J. Environ. Eng. Div. 103, 615–624.

Rees, D.G., 1985. Essential Statistics. Chapman & Hall, London.

Robbins, E.I., Cravotta, C.A., Savela, C.E., Nord Jr., G.L., 1999. Hydrobiogeochemical Interactions in 'anoxic' limestone drains for neutralisation of acidic mine drainage. Fuel 78, 259–270.

Rose, W.A., 2006. Long-term performance of vertical flow ponds – an update. In: Proceedings of the Seventh International Conference on Acid Rock Drainage, St. Louis, Missouri, pp. 1704–1716.

Scheidegger, A., Borkovec, M., Sticher, H., 1993. Coating of silica sand with goethite; preparation and analytical identification. Geoderma 58, 43–65.

Schueck, J.H., Helfich, D.R., Fromell, D.J., 2004. Limestone upflow pond with siphon discharge design considerations – a simple solution to high volume, high metals AMD discharges. In: Proceedings of the Sixth Annual Statewide Conference on Abandoned Mine Reclamation, Western Pennsylvania Coalition for Abandoned Mine Reclamation.

Schwertmann, U., Friedl, J., 1998. Thin iron oxide films on pebbles in ferriferrous streams. N. Jb. Miner. Mh. 2, 63–67.

Schwertmann, U., Taylor, R.M., 1972. The transformation of lepidocrocite to goethite. Clay Clay Min. 20, 151–158.

Singer, P., Stumm, W., 1970. Acid mine drainage: the rate-determining step. Science 167, 1121–1123.

Sterner, P., Skousen, J., Donovan, J., 1998. Geochemistry of laboratory anoxic limestone drains. In: Proceedings of the 15th Annual National Meeting of the American Society for Surface Mining and Reclamation, American Society for Surface Mining and Reclamation, Princeton, WV, pp. 214–234.

Sun, Q., 2000. Iron and acid removal from acid mine drainage in open limestone systems Morgantown, WV, Ph.D. Thesis.

Taylor, J., Waters, J., 2003. Treating ARD – how, when, where and why. Mining Environ. Manage 11, 6–9.

Turner, D., McCoy, D., 1990. Anoxic alkaline drain treatment system, a low cost acid mine drainage treatment alternative. In: Graves, D.H., DeVore, R.W. (Eds.), Proceedings of the 1990 National Symposium of Mining. University of Kentucky, Lexington, KY, pp. 73–75.

Vinci, B.J., Schmidt, T.W., 2001. Passive, periodic flushing technology for mine drainage treatment systems. In: Proceedings of the Sixth Annual Statewide Conference Abandoned Mine Reclamation, Albuquerque, New Mexico, American Society for Surface Mining and Reclamation, pp. 611–625.

Weaver, K.R., Lagnese, K.M., Hedin, R.S., 2004. Technology and design advances in passive treatment system flushing. In: Proceedings of the 2004 National Meeting of the American Society of Mining and Reclamation and the 25th West Virginia Surface Mine Drainage Task Force, American Society of Mine Reclamation, pp. 1974–1989.

Webb, J.A., Sasowsky, I.D., 1994. The interaction of acid mine drainage with a carbonate terrane: evidence from the Obey River, north-central Tennessee. J. Hydrol. 161, 327–346.

Ziemkiewicz, P.F., Brant, D.L., Skousen, J.G., 1996. Acid mine drainage treatment with open limestone channels. Passive treatment systems and improvement of water quality. In: Proceedings of the 17th West Virginia Surface Mine Drainage Task Force Symposium, Morgantown, WV, pp. M-1–M-15.

Ziemkiewicz, P.F., Skousen, J.G., Brant, D.L., Sterner, P.L., Lovett, R.J., 1997. Acid mine drainage treatment with armored limestone in open limestone channels. J. Environ. Qual. 26, 1017–1024.